General outlook of the elaboration of nitrogen doped graphenic materials from the reaction between an amino alcohol and metallic sodium

Lilian Moumaneix, Sébastien Fontana, François Lapicque, Claire Hérold

Title:

General outlook of the elaboration of nitrogen doped graphenic materials from the reaction between an amino alcohol and metallic sodium

Authors:

Lilian Moumaneix,[a] Sébastien Fontana,[a] François Lapicque,[b] and Claire Hérold [*a]

Abstract:

Nitrogen-doped graphenic materials (N-Gr) are attracting increasing interest in the field of electrocatalysis, where their applications as noble metal-free catalysts or as catalyst supports are explored worldwide. Solvothermal-based processes are an efficient way to produce large quantities of N-Gr, without compromising their valuable properties. Reported in earlier publications, our elaboration route is based on a solvothermal reaction between various organic alcohols, e.g. cyclohexanol, ethanolamine, 1-(2-hydroxyethyl)piperidine, and metallic sodium, followed by a pyrolysis treatment under nitrogen flow. Rarely investigated in the literature mainly due to their complex mechanisms, the understanding of such processes opens many paths to tailor the properties of N-Gr, leading to high porosity (> 2200 $m^2.g^{-1}$), good crystallinity, high purity, etc. The present article focuses on the influence of the solvothermal reaction experimental parameters on the final N-Gr, i.e. temperature, pressure, and sodium content. The elaborated materials are studied through multi-scale and complementary characterizations techniques, i.e. Raman spectroscopy, thermogravimetric analysis, X-ray photoelectron spectroscopy, N_2 adsorption at 77 K. An overview of the whole process follows the experimental part, giving quick access to optimized experimental parameters depending on the desired N-Gr properties, e.g. yield, crystallinity or porosity. By way of illustration, some trends were evidenced, such as (i) the larger conversion rate of solvent into crystalline carbon material as the reaction temperature is increased (300 – 380 °C), (ii) the increase of the surface area and the larger nitrogen content with increasing pressure (100 – 200 bar), and (iii) the beneficial impact of the sodium content on the yield and the material crystallinity (Na/solvent ratio 1 – 2).

Keywords:

Solvothermal-based process, nitrogen-doped graphenic materials, chemical mechanism investigations, spectroscopy, microporous materials

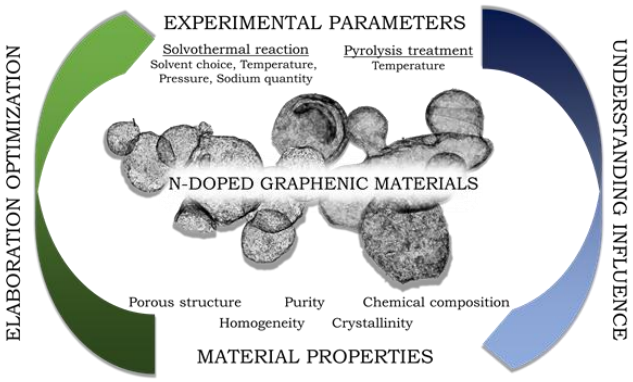

(a) Institut Jean Lamour, CNRS – Université de Lorraine, 2 allée André Guinier, 54011 Nancy, France.

(b) Laboratoire Réactions et Génie des procédés, CNRS – Université de Lorraine, ENSIC, 54000 Nancy, France.

* Corresponding author: Dr. Claire Herold, claire.herold@univ-lorraine.fr +33372742537

1. Introduction

Large scale production of nitrogen-doped graphenic materials (N-Gr), which gather very large surface area (up to 2200 $m^2.g^{-1}$), high electric conductivity and good crystallinity, represents a challenge for the field of energy conversion, and more especially for fuel cells operating at low temperatures. This type of material presents significant activity towards the oxygen reduction reaction (ORR) in both acidic and alkaline media [1-16], and can also provide nucleation sites for metal nanoparticles, increasing notably their dispersion and stability, leading to higher catalytic properties [17-20].

Recently, our group has worked on a solvothermal-based process to elaborate N-Gr [21]. Although studied here at the lab scale, the solvothermal reaction between an alcohol and sodium as well as the following pyrolysis treatment, could be easily up-scaled to recover larger amounts of materials.

In a recent study, our group reported the mechanisms involved during the solvothermal reaction between 1-(2-hydroxyethyl)piperidine (subsequently noted HEP) and metallic sodium [22]. It was evidenced that the early formation of gaseous molecules such as CH_4, NH_3 or CO_2 leads to subsequent reactions with sodium, resulting in the formation of various sodium compounds, e.g. Na_2CO_3, NaH, and NaCN. In addition to that, the solid carbon-rich phase starts its rearrangement into a hexagonal sp^2 network and macromolecules containing aromatic cycles and π-conjugated bonds.

In the present paper, the influence of the solvothermal parameters on the final N-Gr has been studied. Relations between the solvothermal products composition and the evolution of the graphenic materials properties have been drawn out, allowing a better understanding of the whole process. Recommendations concerning the experimental parameters conclude the paper, allowing the reader to easily optimized various properties of the carbon phase, such as its crystallinity, its porous structure, or its homogeneity.

2. Materials and methods

2.1. Solvothermal reactions between metallic sodium and HEP

Under inert atmosphere (N_2, Air Liquide, Alphagaz 2), a mixture of 23 mL (0.17 mol) of 1-(2-hydroxyethyl)piperidine (ACROS organics, 99%) was put into contact with metallic sodium (Merck Millipore), whose mass was chosen to reach the desired sodium/HEP ratio, i.e. 3.91 g (ratio = 1), 5.87 g (ratio = 1.5) or 7.82 g (ratio = 2). The reagents were inserted inside a 0.5 L Parr autoclave, which was then hermetically sealed. Nitrogen (Air Liquide, Alphagaz 2) was injected inside the sealed autoclave so that the internal pressure reaches its targeted value at the reaction temperature, either 100 bar or 200 bar. Finally, the reactor was heated at 300 °C, 350 °C or 380 °C, at 8 $°C.min^{-1}$. The mixture was let to react during 72 h, before turning off the heating system and allowing the autoclave to cool down to room temperature. The solvothermal product was recovered and stored under nitrogen atmosphere, due to its sensitivity to air.

2.2. Pyrolysis treatments of the solvothermal products

About 5 g of solvothermal product was placed in an Inconel® 600 crucible and then introduced in a vertical tubular oven. Depending on the planned conditions, the oven was heated at a heating rate of 20 $°C.min^{-1}$ up to the reaction temperature in the range 750 – 900 °C for 4 h, then cooled down to room temperature naturally. The crucible was permanently kept under a nitrogen flow (Air Liquide, Alphagaz 1) to avoid the combustion of the carbonaceous phase and eliminate the pyrolysis gases. At this stage, the product consists of a greyish black powder.

2.3. Washing of the N-doped graphenic materials

The pyrolysis product was crushed then sonicated 10 min in 200 mL of distilled water. The powder was washed alternatively with 1 L 6 $mol.L^{-1}$ of hydrochloric acid (Sigma Aldrich, $\geqslant$37%) and 1 L of distilled

water. The initially grey powder turned to black due to the removal of sodium carbonate and sodium hydroxide formed during the pyrolysis. The sample was finally dried at 100 °C for 24 h and stored under air.

The yield of the pyrolysis treatment is defined as the ratio of the mass submitted to pyrolysis and the mass recovered after the washing treatment.

Table 1 gathers the conditions of elaboration for the materials studied in this work.

Table 1: Elaboration conditions of the characterized samples; solvothermal reaction pressure is given at the temperature of reaction; reaction time = 72 h.

Sample ID	Solvothermal reaction temperature (°C)	Solvothermal reaction pressure (bar)	Na/HEP molar ratio	Pyrolysis temperature (°C)
N-Gr/S300	**300**	200	1.5	850
N-Gr/S350	**350**	200	1.5	850
N-Gr/S380	**380**	200	1.5	850
N-Gr/Pr100	380	**100**	1.5	850
N-Gr/Pr200	380	**200**	1.5	850
N-Gr/R1.0	350	200	**1.0**	850
N-Gr/R1.5	350	200	**1.5**	850
N-Gr/R2.0	350	200	**2.0**	850
N-Gr/P800	380	200	1.5	**800**
N-Gr/P850	380	200	1.5	**850**
N-Gr/P900	380	200	1.5	**900**

Raman spectroscopy investigations were conducted with a Renishaw inVia Quontor equipped with a 532 nm laser operating in the spectral range 100–3600 cm^{-1} in synchroscan mode. Samples were first dispersed in absolute ethanol then deposited on a glass slide.

X-ray photoelectron spectroscopy (XPS) analysis were achieved with a Kratos Axis Ultra DLD, using an Al $K_{\alpha 1}$ X-ray source (1486.6 eV). C–C and C–H bounds were taken as C 1s signal references at 284.6 eV. Analyzed surface is of 700 x 300 μm^2 for 5–10 nm deep.

Physisorption of nitrogen at 77 K was performed with a Micromeritics ASAP2020 adsorption apparatus. The samples were outgassed 12 h at 300 °C before analysis. Specific surface areas were calculated using the BET (completed with the Rouquerol correction) and the 2D-NLDFT models The micropore volumes and pore size distributions were obtained using the 2D-NLDFT model: this model can actually avoid overestimation of the specific surface area by the BET model for microporous solids. 2D-NLDFT calculations were carried out using the software SAIEUS, with a corrugation parameter $\lambda = 4.25$ and an integration range from 0.4 nm to 29.3 nm.

Thermogravimetric analysis (TGA) were carried out under dry air in a Setsys Evolution Setaram thermobalance. Samples were heated at 1000 °C in a platinum crucible with a heating rate of 3 $°C.min^{-1}$ then cooled down to room temperature at 20 $°C.min^{-1}$. Accuracy in the masses is close to 0.1%.

3. Results and discussion

3.1. Influence of the pyrolysis temperature

The influence of the pyrolysis temperature on the N-doped graphenic materials properties has been reported in a previous publication [21]. However, the solvents mix used for this first study was composed

of a stoichiometric mixture of cyclohexanol and ethanolamine, instead of HEP. In this first part, we aimed to show that the observations realized previously are still valid despite the change in the reagents, and more generally, that the phenomena associated with the pyrolysis temperature can be generalized to other similar carbon-based organic solvents.

Three samples have been characterized, corresponding to three different pyrolysis temperatures, i.e. 800 °C, 850 °C and 900 °C. The conditions of the solvothermal reaction are kept identical, i.e. temperature of 380 °C, pressure of 200 bar and Na/HEP ratio of 1.5 (cf. Table 1).

The yield of the pyrolysis treatment varies from 3.5 wt.% for N-Gr/P850 to 0.6 wt.% for N-Gr/P900. This decrease in the yield was expected due to the larger consumption of the carbon phases at higher pyrolysis temperature.

The TGA measurements displayed in fig. 1 indicate a modification of the homogeneity and the purity of the carbon-phase within the samples. With an increase in the pyrolysis temperature, the peak related to the combustion of the carbon phases, usually appearing between 350 °C and 600 °C, shifts towards lower temperature, from 536 °C for N-Gr/800 to 411 °C for N-Gr/900. This first observation can be associated with the increase in the concentration of sodium compounds inside the materials, which are known to catalyze the combustion of carbon materials [23]. Additionally, the combustion of sodium compounds is visible between 600 °C and 800 °C (figure 1 (a)). The intensity of the related combustion peaks rises with the increase in temperature, validating the increase in the concentration of sodium compounds inside the materials. XPS measurements, not shown here, further confirm this tendency, the atomic quantity of sodium increasing from possible traces to 1.5 at.% for N-Gr/P800 and N-Gr/P900 respectively.

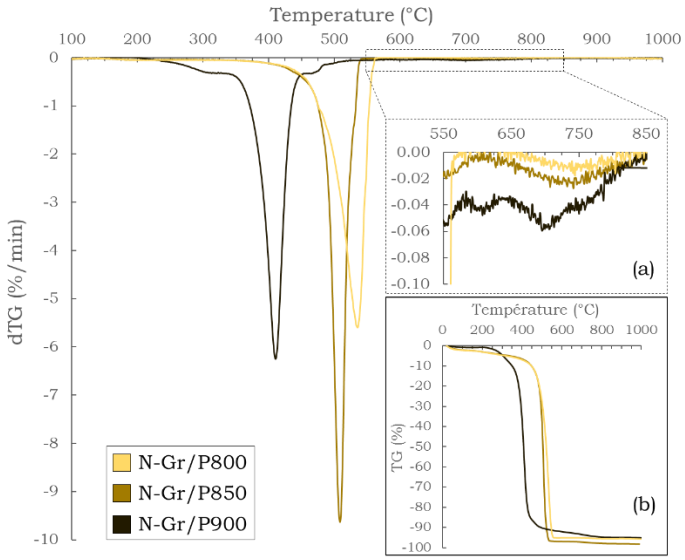

Figure 1: dTG of samples N-Gr/P800 – N-Gr/P900 (dry air, heating rate 3 °C.min^{-1}); (a) focus on the 550-850 °C zone; (b) global TG signal.

The variation of the impurity rates, measured at 600 °C (fig. 1 (b)), i.e. after the combustion of the carbon phases, and the full widths at half maximum (FWHM) of the carbon-related combustion peaks is similar to the one previously reported for other solvents [21]. The pyrolysis temperature of 850 °C seems to be optimal both in terms of purity and homogeneity of the carbon phases (fig. 2), as both the impurity rate and the FWHM reach a minimum at 3.1 wt.% and 20.6 °C respectively.

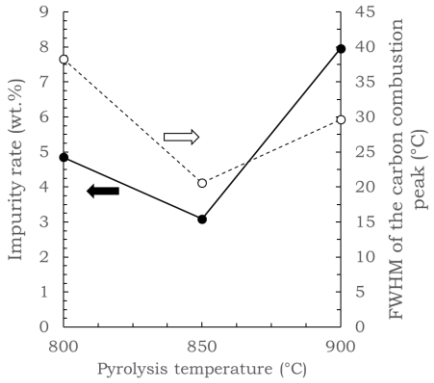

Figure 2: Impurity rate (black dotes) and FWHM of the carbon combustion peak (white dots) measured from TG analysis.

Raman spectroscopy analysis allowed to precise the state of crystallinity of the carbon phases as well as the defects fraction. The spectra presented in figure 3 (a) display a progressive reduction in the width of the D and G bands, located at 1350 cm^{-1} and 1580 cm^{-1} respectively [24-26], associated with a diminution of the defects bands intensity, namely T band at 1100 cm^{-1} [27, 28], F band at 1500 cm^{-1} [28, 29] and D' band at 1620 cm^{-1} [30] (fig. 3 (c)). The gradual rise in the G' band, located around 2700 cm^{-1} [24, 31], tends to show that the stacking order of the graphene layers along the $\vec{c}$ axis increases with the pyrolysis temperature. The crystallites size La [32], indicator of the in-plane graphene layers crystallinity, can be followed by looking at both the I_D/I_G ratio and the FWHM of the G band (noted subsequently FWHM (G)). These two parameters, plotted figure 3 (b), present similar variations and can therefore be correctly interpreted. As the pyrolysis temperature increases from 800 °C to 850 °C, I_D/I_G ratio diminishes from 1.31 to 1.06, indicating an increase in material crystallinity, expected for this kind of heat treatment. Further increase in the pyrolysis temperature to 900 °C generates a low variation of the I_D/I_G ratio and the FWHM (G), implying the presence of a phenomenon whose action opposites the one of crystallinity. Previously noticed for other solvents [21], high pyrolysis temperatures are believed to lead to degradations of the carbon phases, thus limiting the overall crystallinity of the graphenic materials.

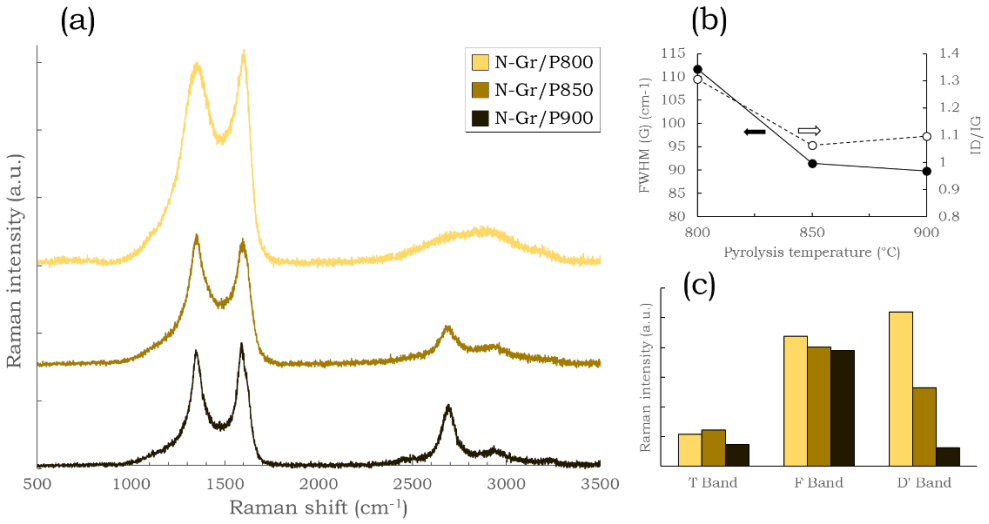

Figure 3: (a) Raman spectra of samples N-Gr/P800 – N-Gr/P900; (b) evolution of the FWHM (G) (black dots) and the I_D/I_G ratio (white dots) with the pyrolysis temperature; (c) Raman intensities of the T, F and D' bands.

Through this brief description of the graphenic-materials properties along with the pyrolysis temperature, we aim to show that similar behaviors can be expected for solvothermal-based processes, even with changes in the chosen solvent(s).

3.2. Influence of the solvothermal reaction temperature

Variations in the graphenic materials properties have been studied with the evolution of the solvothermal reaction parameters. Correlations with the known mechanisms intervening during this reaction (described in [22]) are of great use to further optimize the synthesis, leading to graphenic materials with desired properties.

The influence of the solvothermal reaction temperature has been investigated between 300 °C and 380 °C, with an intermediary value at 350 °C, corresponding to samples N-Gr/S300, N-Gr/ S350 and N-Gr/S380 respectively (cf. Table 1). The yield of the pyrolysis treatment exhibits an important increase with the elevation of the solvothermal reaction temperature (fig. 4), from 1.2 wt.% for N-Gr/S300 to 3.5 wt.% for N-Gr/S380. The pyrolysis temperature remaining identical for all the samples (850 °C), this increase could be linked to an enrichment of the intermediary solvothermal product in solid compounds capable of leading to a carbon structure after pyrolysis. In addition, changes in the solvothermal product aspect were previously noted with an increase in the solvothermal reaction temperature [22], turning from oily to dry, and from dark brown to black. Therefore, the solvothermal reaction could act as a pre-pyrolysis treatment that favors rearrangement reactions of the carbon phases, its action getting stronger as the temperature increases.

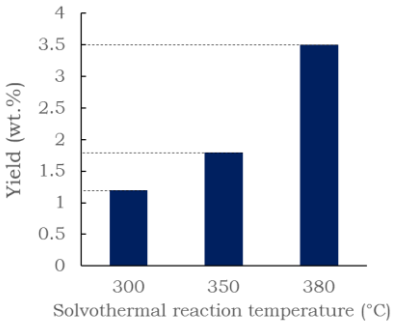

Figure 4: Variation of the yield of pyrolysis treatment with the solvothermal reaction temperature.

Raman spectroscopy characterizations indicate that the quantity of defects inside the graphenic materials remains quite constant for the three samples investigated (fig. 5 (a)). However, the increase in the G and G* bands (figure 5 (b)) (the latter being a harmonic of the G band, located around 3200 cm^{-1} [33], and used here to confirm the tendency of the G band) as well as the G' band (figure 5 (c)), exposes an enhancement of the overall N-Gr crystallinity. This observation corroborates the hypothesis previously made about the rearrangement of carbon atoms during the solvothermal reaction, since it would very likely have an associated impact on the materials crystalline state.

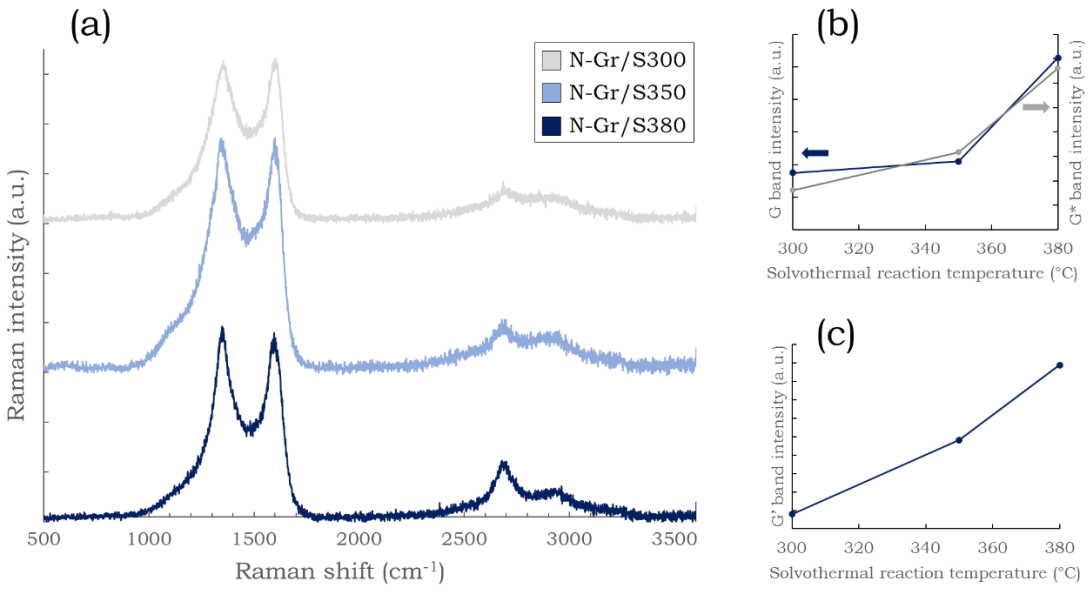

Figure 5: (a) Raman spectra of samples N-Gr/S300 – N-Gr/S380; (b) evolution of the Raman intensities of the G and G bands; (c) evolution of the Raman intensity of the G' band.*

The chemical composition of the samples, measured by XPS, reveals that for the lowest solvothermal reaction temperature, i.e. 300 °C, the quantity of oxygen atoms is higher than in the other samples, to the detriment of carbon atoms, from 6.5 at.% for N-Gr/S300 to about 3.3 at.% for N-Gr/S380 (fig. 6). This finding might explain the enrichment of the intermediary solvothermal product in carbon-based structures, from the elimination of oxygen functions at the highest reaction temperatures, in the form of H_2O or CO_2 for example.

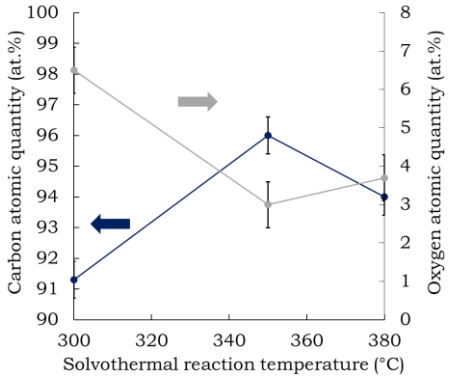

Figure 6: Variation of the carbon (blue dots) and oxygen (grey dots) atomic quantities measured by XPS with the solvothermal reaction temperature.

The investigations carried out on the influence of the solvothermal reaction temperature on the final N-Gr, led to the conclusion that this parameter is mainly involved in the rearrangement of the carbon atoms into a hexagonal conjugated network, as it has been evidenced in our previous study [22]. This pre-pyrolysis treatment has a direct impact on the crystallinity of the final materials as well as the yield of the pyrolysis treatment.

3.3. Influence of the solvothermal reaction pressure

Two pressures for the solvothermal reaction have been studied in this work: 100 bar and 200 bar, corresponding to samples N-Gr/P100 and N-Gr/P200 respectively (cf. Table 1). During a solvothermal reaction, the pressure can principally act according to three effects [34]: (i) the energy conveyed by the

pressure on the reactional environment; (ii) the compression effect; (iii) the induced chemical reactivity. The energy resulting from the application of pressure is directly correlated to the compressibility of the considered medium. If this energy can reach fairly high values for gas, the energy transmitted to liquid or solid is negligible. In all cases, the amount of energy brought by the pressure is far lower than the one needed for a chemical reaction [34].

According to the Le Chatelier's principle, the compression of a certain medium favors the reactions leading to a diminution of the overall quantity of chemical entities in this medium. This effect can play an important role as it allows the formation of denser structures, as well as shifting reactional equilibria. Moreover, with a rise in pressure, an increase in the solubility of solvated species and a decrease in the average distance between them is usually seen [34].

The influence of the reaction pressure on the N-Gr has been firstly investigated with N_2 adsorption measurements at 77 K. The experimental isotherms (fig. 7 (a)) present the aspects of type I(b) and type IV(a) isotherms, as classified in the IUPAC's recommendations [35]. These typical behaviors are related to porous materials, containing a large fraction of micropores (< 2nm in diameter) and some wider mesopores (2-5 nm in diameter). No significant change is noticeable between the two pore size distributions displayed in figure 7 (b), the modification of pressure does not imply the formation of a new population of pores. However, a reduction of the total pore volume, from 0.77 $cm^3.g^{-1}$ to 0.69 $cm^3.g^{-1}$, can be seen with the increase of pressure from 100 bar to 200 bar (figure 7 (c)). This behavior corresponds to a decrease in both the microporous and mesoporous volumes, likely resulting from a compression effect, the lower pressure imposing less mechanical stress over the carbon-based network than the higher one, therefore allowing lighter structures.

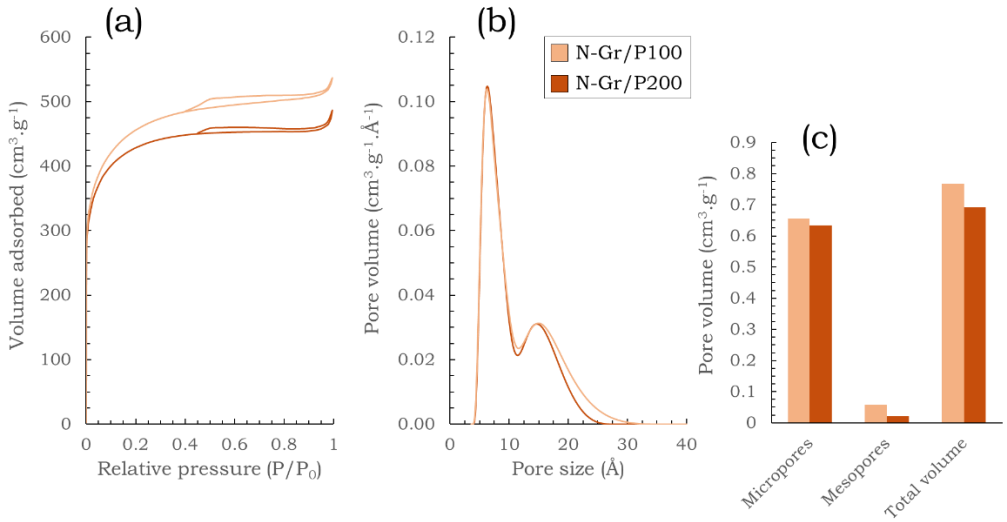

Figure 7: (a) Adsorption isotherms (N_2, 77 K) of samples N-Gr/P100 and N-Gr/P200; (b) distribution of the pore volumes with the pore sizes; (c) microporous, mesoporous and global porous volumes.

The crystallinity of samples N-Gr/P100 and N-Gr/P200 has been investigated via Raman spectroscopy (fig. 8 (a)). Considering the spectra recorded on different areas for each sample, I_D/I_G ratios and FWHM (G) display similar values, around 1.1 and 92 cm^{-1} respectively. The average intensity of the defect bands T, F and D' also shows comparable values. However, N-Gr/P200 presents a pronounced G' band at 2700 cm^{-1}, along with a slight increase in the intensity of the G and G* bands (figure 8 (b)), resulting from a better stacking of the graphene layers. This result tends to indicate that the pressure inside the

solvothermal reactor plays a role in the organization of the carbon-based particles, leading after the pyrolysis treatment to better crystallized N-Gr.

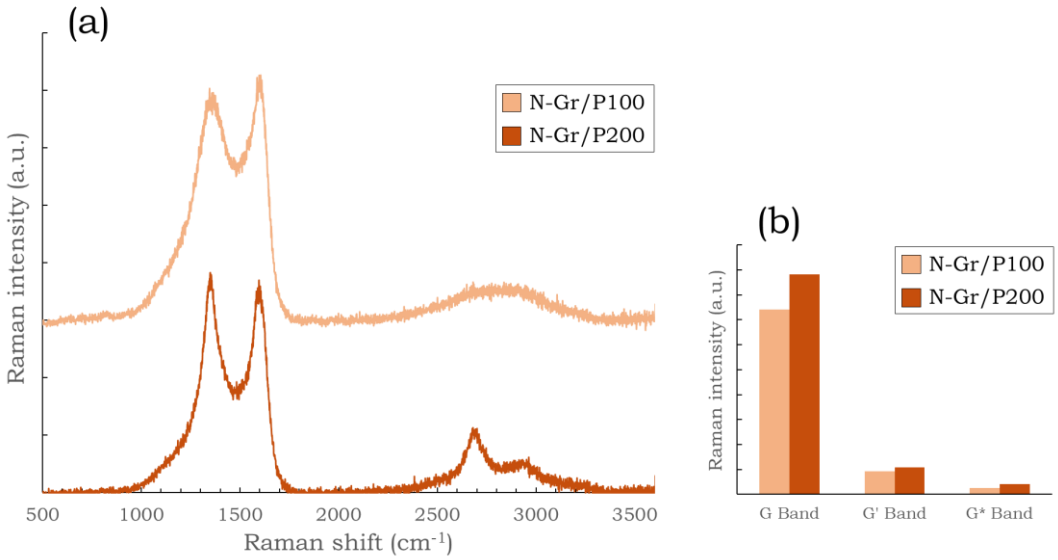

Figure 8: (a) Raman spectra of samples N-Gr/S300 – N-Gr/S380; (b) evolution of the Raman intensities of the G, G' and G bands.*

If the C, O and Na content for both materials remains at a steady level, i.e. 94.4 at.%, 3.8 at.% and 0.2 at.% respectively, the quantity of nitrogen atoms rises with the increase in pressure, from 0.9 at.% for N-Gr/P100 to 1.9 at.% for N-Gr/P200. This increase could be explained by a compression effect, and more specifically from a shift in the reactional equilibria towards the formation of lesser number of molecules. In our previous work [22], we showed that methanation reactions as well as other reactions were likely to happen during the solvothermal process, leading to the formation of solid state nitrogen compounds. Equations (1) to (3) give a possible route to explain the observed behaviour:

$$CO + 3H_2 \rightleftharpoons CH_4 + H_2O \qquad \text{Equation 1}$$

$$CO_2 + 4H_2 \rightleftharpoons CH_4 + 2H_2O \qquad \text{Equation 2}$$

$$N_2 + 3H_2 \rightleftharpoons 2NH_3 \qquad \text{Equation 3}$$

According to the compression effect, it appears that the formation of CH_4 and NH_3 from the reactions (1) – (3) is favored by high pressure due to the decrease in the overall number of molecules. Since these two molecules are likely to be involved in the formation of solid nitrogen compounds according to reactions (5) and (6), we can suppose that the higher the pressure the higher the quantity of nitrogen in the solid phase. During the pyrolysis treatment, NaCN or $NaNH_2$ could be decomposed, and nitrogen atoms could migrate inside the carbon network. Reaction pressure beyond 200 bar may further enhance this effect and improve the N-doping.

$$CH_4 + NH_3 \rightleftharpoons HCN + 3H_2 \qquad \text{Equation 4}$$

$$HCN + NaOH \rightleftharpoons NaCN + H_2O \qquad \text{Equation 5}$$

$$Na + NH_3 \rightleftharpoons NaNH_2 + 1/2H_2 \qquad \text{Equation 6}$$

3.4. Influence of the Na/HEP molar ratio

The last parameter investigated was the Na/HEP molar ratio, for three different values: 1.0, 1.5 and 2.0, corresponding to samples N-Gr/R1.0, N-Gr/R1.5 and N-Gr/R2.0 respectively (cf. Table 1). The yield of pyrolysis greatly increases with the increase in the sodium quantity, from 0.6 wt.% for N-Gr/R1.0 to 4.7 wt.% for N-Gr/R2.0 (cf. figure 9). It is important to notice that despite the different quantities of sodium inserted in the solvothermal reactor, the final materials exhibit similar Na contents, around 0.5±0.2 at.%. Therefore, the increase in pyrolysis yield can be attributed to a higher proportion of carbon-based structure.

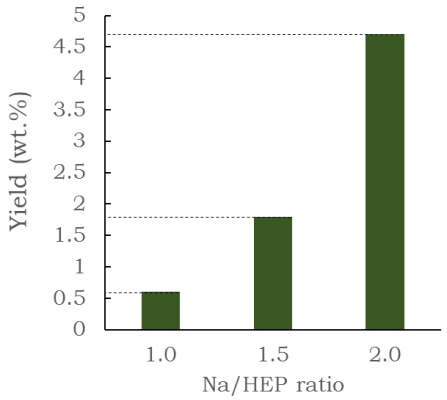

Figure 9: Evolution of the yield of the pyrolysis treatment with the Na/HEP molar ratio.

The increase in the Na/HEP ratio is also responsible for a variation of the C/O ratio in the final N-Gr, as shown in figure 10. The fraction of carbon atoms increases from 92 at.% to 96 at.% with the increase in Na/HEP ratio, while the fraction of oxygen atoms diminishes from 6 at.% to 2 at.%.

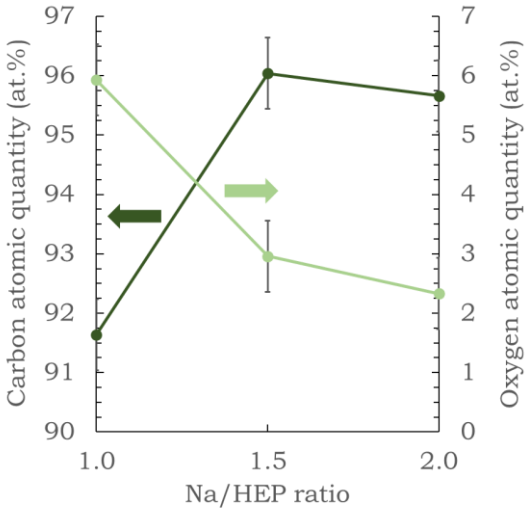

Figure 10: Variation of the carbon (dark green dots) and oxygen (light green dots) atomic quantities measured by XPS with the Na/HEP molar ratio.

From these two observations, it can be concluded that sodium atoms are involved in a large number of reactions, able to modify the chemical composition of the solid phase. The high reactivity of sodium could explain the decrease in the fraction of oxygen atoms, since sodium can easily react with oxygenated molecules, e.g. H_2O or CO_2, to form solid sodium compounds, e.g. NaOH or Na_2CO_3, which can be washed away with ease during the acidic washing of the N-Gr, resulting in a diminution of the O content.

Reactions with oxygen functions located at the surface of the carbon-based structure can also be imagined.

Moreover, sodium atoms are involved in reactions with carbon-containing molecules, e.g. CH_4 (eq. 4-5) or CO_2, which could act as a storage of carbon atoms in a solid state, e.g. NaCN or Na_2CO_3, enhancing the transfer of carbon atoms from the solvothermal reaction to the pyrolysis treatment. Without such process, a large proportion of carbon atoms would be lost during the opening of the solvothermal reactor in the form of CH_4, NH_3, CO_2, HCN or other small molecules. This hypothetical mechanism could partly explain the noticeable increase in the pyrolysis yield. A second idea comes from the evaluation of the graphenic materials crystallinity.

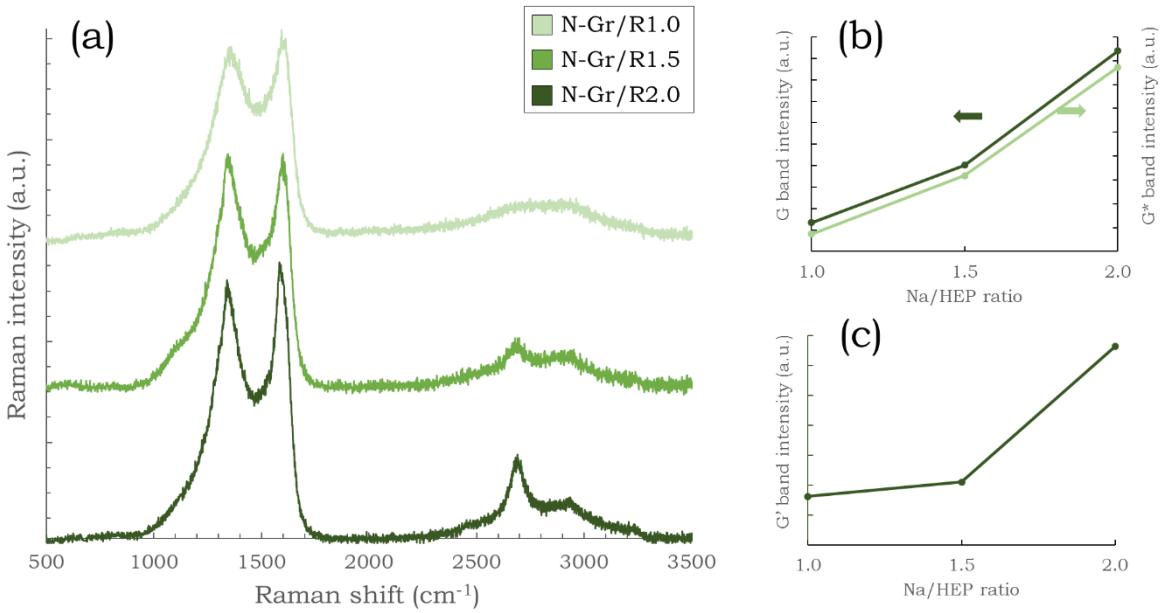

Figure 11: (a) Raman spectra of samples N-Gr/R1.0 – N-Gr/R2.0; (b) evolution of the Raman intensities of the G and G bands; (c) evolution of the Raman intensity of the G' band.*

Looking at the Raman spectra measured for the three samples (fig. 11 (a)), one can notice that an increase in the Na/HEP ratio participates to the improvement of the overall crystallinity of the carbon phase. Indeed, the intensities of both G and G* bands follow an upwards evolution (fig. 11 (b)), a similar behavior being also observed for the G' band (fig. 11 (c)). The reducing properties of sodium and other sodium compounds such as NaH could actively favor elimination reactions during the solvothermal reaction, resulting in larger fractions of conjugated and highly stable carbon networks, therefore improving the crystallinity and the thermal stability of the carbon phase.

Even though Na/HEP ratios higher than 2 have not been investigated, the trends evidenced here are likely to remain valid for higher quantities of Na inserted into the solvothermal reactor. However, this cannot carry on indefinitely as these trends are the result of reactions between Na and other molecules, the latter being consumed in the process. Additionally, some unexpected phenomenon could take place if the composition of the gas and solid phases changes a lot due to the insertion of Na in large excess.

3.5. Discussion around the optimization of graphenic materials properties

The multitude of measurements done up to now allow us to have a detailed overview, even if not exhaustive, of the influence of different experimental parameters on the N-Gr properties. Global trends have been discerned, clarifying the solvothermal-based process, simple in its implementation, but

complex in its numerous reactional mechanisms. This part aims to bring recommendations concerning the choice of the experimental parameters, in order to optimize the graphenic material desired properties.

3.5.1. Yield of synthesis

The yield of synthesis, calculated as the mass ratio between the mass of solvothermal product submitted to the pyrolysis treatment and the mass of N-doped graphenic material recovered after the washing step, is mainly impacted by the chemical composition of the samples.

Previously reported in part 3.2., the higher the solvothermal temperature the higher the yield of synthesis, within the studied range (300-380 °C). This increase could be ascribed to the better organization of carbon atoms inside the samples treated at high temperatures, resulting in higher thermal stabilities.

The Na/solvent molar ratio presents a great influence on the yield of synthesis, the highest yield being obtained for the highest Na/solvent ratio. Several hypothesis have been proposed in part 3.4.: (i) the higher rate of elimination reactions, favored by reductant media, resulting in a higher fraction of double-bounded C=C; (ii) the storage of carbon atoms in the form of sodium compounds such as NaCN or Na_2CO_3; (iii) the decrease in oxygen atom quantity, leading to fewer oxidation reactions during the pyrolysis treatment. Whatever the mechanism involved, it has to be noticed that the increase in the yield of synthesis is not related to an increase in the sodium compound quantities in the final materials, which remain constant around 0.5 at.% in all samples.

The pyrolysis temperature also plays an important role, an increase in temperature resulting in a dramatic decrease in the yield of synthesis. This observation takes into consideration the present publication as well as our previous work [21]. At 900 °C and above, the synthesis yield becomes so low (< 1 wt.%) that it cannot be considered as an efficient way to produce N-doped graphenic materials.

3.5.2. Homogeneity and purity of the carbon phase

The homogeneity and purity of the carbon phase in the graphenic materials are mainly influenced by the pyrolysis treatment. It has been exposed that, no matter the solvent(s) used, the pyrolysis temperature of 850 °C gives the highest purity and homogeneity. At this temperature, no major thermal degradation occurs yet, resulting in low quantities of impurities and few different carbon phases. If the influence of the solvothermal reaction on the homogeneity and the purity of the carbon phase is not considered as null, no general trend has been evidenced yet.

3.5.3. Crystallinity of the carbon phase

The crystallinity of the N-Gr still remains difficult to quantify properly at the macroscopic scale due to the presence of several carbon phases. However, qualitative analysis from Raman spectroscopy measurements allowed to point out general trends. From preliminary works not presented here, it has been evidenced that linear molecules used as solvents, e.g. ethanol mixed with ethanolamine, do not permit the elaboration of a well-ordered carbon network, the materials remaining mainly amorphous. The choice of the solvents can then be considered as a critical parameter to reach high crystallinity, using single-bounded hexagonal rings, such as cyclohexanol or 1-(2-hydroxyethyl)piperidine, is therefore recommended.

An increase in the solvothermal reaction temperature, pressure or Na/solvent ratio results in an improvement of the overall crystallinity, as developed in the previous paragraphs. However, the intensities of the defect bands seen in Raman spectra, e.g. T, F and D' bands, remain quite stable

regardless of the solvothermal reaction conditions. Therefore, it can be proposed that the solvothermal reaction mainly influence the stacking of preexisting graphenic domains, while its impact on the conversion of amorphous carbon fractions into ordered phases is quite limited.
In the other hand, the pyrolysis temperature has a greater influence on the crystallinity of the carbon phase. It has been shown that the higher the pyrolysis temperature the higher the crystallinity. Moreover, the decrease in intensities of the Raman defects bands implies a crystallization of amorphous carbon phases. However, thermal degradation can occur for temperatures higher than 850 °C, limiting the reachable crystallinity.

3.5.4. Textural properties and porous structure

The textural properties of N-Gr are principally characterized by their specific surface areas, their porous volumes, and their pore size distributions. The solvothermal reaction pressure has a significant impact on the surface area as well as the porous volume. A decrease in pressure, from 200 bar to 100 bar, leads to an increase of these two parameters of about 5 % and 12 % respectively.
The pyrolysis temperature exhibits the greatest influence on the porous structure. With an increase in the temperature, from 750 °C to 900 °C, a decrease in the surface area of 36 % has been observed, from 2195 $m^2.g^{-1}$ to 1607 $m^2.g^{-1}$ [21]. In the same temperature range, the pore size distribution is modified, resulting mainly in microporous materials at low temperatures, to materials containing a larger population of mesopores, macropores and non-porous surfaces at high temperatures. This variation can be associated with a better stacking of graphene layers, limiting the microporosity accessible between two layers, as well as an increase in the fraction of non-porous graphitic surfaces. Thus, depending on the desired properties, the pyrolysis temperature appears as an easy way to control the porous structure of N-Gr.

3.5.5. Chemical composition

The chemical composition of the N-doped graphenic materials can be of great importance depending on the targeted application. During the synthesis, each experimental parameter has a distinct influence on the overall chemical composition, allowing a fine adjustment of the different quantities of the present atoms.
As the solvothermal reaction temperature increases from 300 °C to 380 °C, the quantities of carbon atoms and oxygen atoms increase and decrease respectively, from about 91 at.% to 95 at.% and from 6.5 at.% to 3.5 at.%. This change could be connected to the higher proportion of well-crystallized carbon phase, more stable during the pyrolysis treatment.
The solvothermal reaction pressure seems to have a limited influence on the chemical composition. However, possibly due to shifts in the reactional equilibria (cf. Part 3.3), the quantity of nitrogen atoms inserted inside the graphenic network greatly increases with the elevation of pressure, from 0.9 at.% at 100 bar to 1.9 at.% at 200 bar.
The quantity of metallic sodium inserted inside the solvothermal reactor, monitored as the Na/HEP molar ratio, has an important impact on the reactions occurring during the synthesis. As a result, the amount of carbon atoms increases with the Na/HEP ratio, from 91.6 at.% to 95.7 at.%, possibly due to their storage in the form of solid sodium compounds such as NaCN. In the meantime, the amount of oxygen atoms decreases, from 5.9 at.% to 2.3 at.%, which could be explained by the high reactivity of oxygen towards sodium. It is important to remember that an increase in the Na/HEP ratio does not imply an increase in the Na content inside the final N-Gr.

Apart from the solvothermal reaction, the pyrolysis treatment also plays an important role in the chemical composition. Interestingly, the higher quantity of carbon atoms as well as the lower quantity of oxygen atoms are obtained for a temperature of 850 °C. As it has been presented in part 3.1, this temperature corresponds to the optimal condition to limit the number of defects in the graphenic material. Thus, the lower amount of oxygen atoms at 850 °C could be linked with the low proportion of carbon defects at this temperature. Indeed, oxygen atoms are principally located on carbon defects and on the carbon network edges. Additionally, the number of nitrogen atoms diminishes with the increase in the pyrolysis temperature, from 2.4 at.% at 800 °C to 1.6 at.% at 900 °C. The low thermal stability of nitrogen surface functions (-NH_3, -CN, etc.) could explain this decrease. As presented in the TGA measurements, the increase in the amount of impurities with the pyrolysis temperature, from traces at 800 °C to 1.5 at.% at 900 °C, should also be considered when choosing the treatment conditions.

Table 2: Simplified overview of the influence of the solvothermal-based process on the final N-doped graphenic material properties

		Yield of pyrolysis	Purity & homogeneity of the carbon phase	Cristallinity of the carbon phase	Surface area	Chemical composition		
						Carbon qty.	Nitrogen qty.	Oxygen qty.
Solvothermal reaction temperature (°C)	380 ↗ 300	↗	-	↗	-	↗	-	↘
Solvothermal reaction pressure (bar)	200 ↗ 100	-	-	↗	↗	-	↗	-
Na/Solvent molar ratio	2.0 ↗ 1.0	↗	-	↗	-	↗	-	↘
Pyrolysis temperature (°C)	900 ↗ 850	↘	↘	→	↘	↘	↘	↗
	↗ 750 [21]	↗	↗	↘	↗	↗	↘	↘

4. Conclusion

The elaboration of nitrogen-doped graphenic materials through a solvothermal-based process allows the recovery of macroscopic quantities of powder, easy to handle, and containing particles with good structural properties. The numerous chemical mechanisms involved during the synthesis give efficient ways to control the overall properties of the materials, e.g. homogeneity, purity, crystallinity, porous structure and chemical composition. In the present paper, it has been shown that, apart from the pyrolysis treatment, the experimental parameters of the solvothermal reaction have a significant influence on the final material properties. A brief summary gathering the principal properties investigated has been proposed, allowing the optimization of a similar process in order to maximize one property or another.

In brief, the present study demonstrated the direct relationship between the solvothermal reaction temperature and the structural organization of the carbon atoms, high temperatures favoring better stackings of the graphenic plans, low O content and higher yields. Additionally, a compression effect was observed, resulting in higher N-doping at 200 bar compared to 100 bar, which we attributed to a shift in gas reaction equilibria. It was also noted that changing the quantity of metallic sodium introduced inside the reactor can help reduce the amount of oxygen atoms in the final N-Gr, as well as increasing the yield and the crystallinity of the carbon phase.

The present work could be extended by studying the influence of the solvothermal duration. Limited here to 72 h for technical reasons, lower durations (24 h) yielded heterogeneous solvothermal products with a

predominant oily phase (not shown here). The conversion of this oily phase to the dry powder recovered here after 72 h could imply an important influence of this parameter on the organization of the carbon-based network, favoring large networks for long reaction durations. In addition to that, the influence of the chosen mix of solvents has not been fully understood yet. If cyclic molecules appeared necessary to obtain well-crystallized graphenic materials, the role of each function and the reactions involved at the beginning of the process remain unclear.

In addition, while giving an experimental guideline to optimize the graphenic material properties, this work could also bring interesting theoretical aspects to help understand solvothermal-based processes, which are rarely studied in the literature.

Conflicts of interest

There are no conflicts to declare.

Acknowledgements

This work was supported partly by the French PIA project "Lorraine Université d'Excellence", reference ANR-15-IDEX-04-LUE.

5. References

[1] Y. Zhang, J. Ge, L. Wang D. Wang, F. Ding, X. Tao, W. Chen, Manageable N-doped Graphene for High Performance Oxygen Reduction Reaction. *Sci. Rep., 2013,* **3**.

[2] L. Zhang, Z. Xia, Mechanisms of Oxygen Reduction Reaction on Nitrogen-Doped Graphene for Fuel Cells. *J. Phys. Chem. C,* 2011, **115**, 11170–11176.

[3] Y. Shao, S. Zhang, M.H. Engelhard, G. Li, G. Shao, Y. Wang, J. Liu, I.A. Aksay, Y. Lin, Nitrogen-doped graphene and its electrochemical applications. *J. Mater. Chem.,* 2010, **20**, 7491.

[4] S.M. Lyth, Y. Nabae, N.M. Islam, T. Hayakawa, S. Kuroki, M. Kakimoto, S. Miyata, Solvothermal Synthesis of Nitrogen-Containing Graphene for Electrochemical Oxygen Reduction in Acid Media. *E-J. Surf. Sci. Nanotechnol.,* 2012, **10**, 29–32.

[5] C. H. Choi, S. H. Park, M. W. Chung, S. I. Woo, Easy and controlled synthesis of nitrogen-doped carbon. *Carbon,* 2013, **55**, 98–107.

[6] R. Ma, X. Ren, B.Y. Xia, Y. Zhou, C. Sun, Q. Liu, J. Liu, J. Wang, Novel synthesis of N-doped graphene as an efficient electrocatalyst towards oxygen reduction. *Nano Res.,* 2016, **9**, 808–819.

[7] H. Kiuchi, H. Niwa, M. Kobayashi, Y. Harada, M. Oshima, M. Chokai, Y. Nabae, S. Kuroki, M. Kakimoto, T. Ikeda, K. Terakura, S. Miyata, Study on the oxygen adsorption property of nitrogen-containing metal-free carbon-based cathode catalysts for oxygen reduction reaction. *Electrochimica Acta*, 2012, **82**, 291–295.

[8] D. Geng, Y. Chen, Y. Chen, Y. Li, R. Li, X. Sun, S. Ye, S. Knights, High oxygen-reduction activity and durability of nitrogen-doped graphene. *Energy Environ. Sci.*, 2011, **4**, 760.

[9] B. Zheng, J. Wang, F.-B. Wang, X.-H. Xia, Synthesis of nitrogen doped graphene with high electrocatalytic activity toward oxygen reduction reaction. *Electrochem. Commun.*, 2013, **28**, 24–26.

[10] P. Yan, J. Liu, S. Yuan, Y. Liu, W. Cen, Y. Chen, The promotion effects of graphitic and pyridinic N combinational doping on graphene for ORR. *Appl. Surf. Sci.*, 2018, **445**, 398–403.

[11] L. Lai, J.R. Potts, D. Zhan, L. Wang, C.K. Poh, C. Tang, H. Gong, Z. Shen, J. Lin, R.S. Ruoff, Exploration of the active center structure of nitrogen-doped graphene-based catalysts for oxygen reduction reaction. *Energy Environ. Sci.*, 2012, **5**, 7936.

[12] M. Florent, R. Wallace, T. J. Bandosz, Oxygen Electroreduction on Nanoporous Carbons: Textural Features vs Nitrogen and Boron Catalytic Centers. *ChemCatChem*, 2019, **11**, 851–860.

[13] J. Huang, J. Han, T. Gao, X. Zhang, J .Li , Z. Li , P. Xu , B. Song, Metal-free nitrogen-doped carbon nanoribbons as highly efficient electrocatalysts for oxygen reduction reaction. *Carbon*, 2017, **124**, 34-41.

[14] D. Geng , Y. Chen , Y. Chen , Y. Li , R. Li , X. Sun , S. Ye , S. Knights, High oxygen-reduction activity and durability of nitrogen-doped graphene. *Energy Environ. Sci.*, 2011, **4**, 760-764

[15] L. Qu , Y. Liu , J-B. Baek , L. Dai, Nitrogen-Doped Graphene as Efficient Metal-Free Electrocatalyst for Oxygen Reduction in Fuel Cells. *ACS Nano*, 2010, **4**, 1321-1326.

[16] Y. Shao , S. Zhang , M.H. Engelhard , G. Li , G. Show , Y. Wang , J. Liu , I.A. Aksay , Y. Lin, Nitrogen-doped graphene and its electrochemical applications. *J. Mater. Chem.*, 2010, **20**, 7491-7496.

[17] R. Imran Jafri, N. Rajalakshmi, S. Ramaprabhu, Nitrogen doped graphene nanoplatelets as catalyst support for oxygen reduction reaction in proton exchange membrane fuel cell. *J. Mater. Chem.*, 2010, **20**, 7114.

[18] X. Chen, D. Deng, X. Pan, Y. Hu, X. Bao, N-doped graphene as an electron donor of iron catalysts for CO hydrogenation to light olefins. *Chem. Commun.*, 2015, **51**, 217–220.

[19] S.R. Chowdhury, T. Maiyalagan, Enhanced Electro-catalytic Activity of Nitrogen-doped Reduced Graphene Oxide Supported PdCu Nanoparticles for Formic Acid Electro-oxidation. *Int. J. Hydrog. Energy*, 2019, **44**, 14808–14819.

[20] A.K. Mageed, A.B. Dayang Radiah, A. Salmiaton, S. Izhar, M. Abdul Razak, Nitrogen doped graphene-supported trimetallic CuNiRu nanoparticles catalyst for catalytic dehydrogenation of cyclohexanol to cyclohexanone. *J. King Saud Univ. - Sci.*, 2019, **31**, 878–885.

[21] L. Moumaneix , S. Fontana , M. Dossot , F. Lapicque , C. Hérold, Nitrogen-doped graphenic foam synthesized by solvothermal-based process: Effect of pyrolysis temperature on the material properties. *Microporous and Mesoporous Mater.*, 2020, **300**.

[22] L. Moumaneix , J. Guerrero Parra , S. Fontana , F. Lapicque , C. Hérold, Investigation of and mechanism proposal for solvothermal reaction between sodium and 1-(2-hydroxyethyl)piperidine as the first step towards nitrogen-doped graphenic foam synthesis. *New J. Chem*, 2020, **44**, 13207-13215. https://doi.org/10.1016/j.micromeso.2020.110165.

[23] L. Speyer, S. Fontana, S. Ploneis, C. Hérold, Influence of the precursor alcohol on the adsorptive properties of graphene foams elaborated by a solvothermal-based process. *Microporous Mesoporous Mater.*, 2017, **243**, 254–262.

[24] L.M. Malard, M.A. Pimenta, G. Dresselhaus, M.S. Dresselhaus, Raman spectroscopy in graphene. *Phys. Rep.*, 2009, **473**, 51–87.

[25] Z. Luo, C. Cong, J. Zhang, Q. Xiong, T. Yu, The origin of sub-bands in the Raman D-band of graphene. *Carbon*, 2012, **50**, 4252–4258.

[26] Cançado, L. G. et al. General equation for the determination of the crystallite size La of nanographite by Raman spectroscopy. *Appl. Phys. Lett*. **88**, 163106 (2006).

[27] S. Piscanec, F. Mauri, A.C. Ferrari, M. Lazzeri, J. Robertson, Ab initio resonant Raman spectra of diamond-like carbons. *Diam. Relat. Mater*., 2005, **14**, 1078–1083.

[28] L. Bokobza, J.-L. Bruneel, M. Couzi, Raman Spectra of Carbon-Based Materials (from Graphite to Carbon Black) and of Some Silicone Composites. *C*, 2015, **1**, 77–94.

[29] A. Bhaumik, A. Haque, M.N.F. Taufique, P. Karnati, R. Patel, M. Nath, K. Ghosh, Reduced Graphene Oxide Thin Films with Very Large Charge Carrier Mobility Using Pulsed Laser Deposition. *J. Mater. Sci. Eng*. 2017, **6**.

[30] A. Eckmann, A. Felten, A. Mishchenko, L. Brinell, R. Krupke, K.S. Novoselov, C. Casiraghi, Probing the Nature of Defects in Graphene by Raman Spectroscopy. *Nano Lett*. 2012, **12**, 3925–3930.

[31] Z. Ni, Y. Wang, T. Yu, Z. Shen, Raman spectroscopy and imaging of graphene. *Nano Res*. 2008, **1**, 273–291.

[32] J. Schwan, S. Ulrich, V. Batori, H. Ehrhardt, S.R.P. Silva, Raman spectroscopy on amorphous carbon films. *J. Appl.* Phys., 1996, **80**, 440–447.

[33] L.G. Bulusheva, A.V. Okotrub, I.A. Kinloch, I.P. Asanov, A.G. Kurenya, A.G. Kudashov, X. Chen, H. Song, Effect of nitrogen doping on Raman spectra of multi-walled carbon nanotubes. *Phys. Status Solidi B*, 2008, **245**, 1971–1974.

[34] G. Demazeau, Impact of high pressures in solvothermal processes. *J. Phys. Conf. Ser.*, 2010,**215**, 012124.

[35] M. Thommes, K. Kaneko, A.V. Neimark, J.P. Olivier, F. Rodriguez-Reinoso, J. Rouquerol, K.S.W. Sing, Physisorption of gases, with special reference to the evaluation of surface area and pore size distribution (IUPAC Technical Report). *Pure Appl. Chem*., 2015, **87**, 1051–1069.